Citation: Molecular Therapy—Nucleic Acids (2013) 2, e129; doi:10.1038/mtna.2013.56

www.nature.com/mtna

Gene Silencing in Skin After Deposition of Self-Delivery siRNA With a Motorized Microneedle Array Device

Robyn P Hickerson[1,2], Winston C Wey[3,4], David L Rimm[5], Tycho Speaker[1], Susie Suh[3], Manuel A Flores[1], Emilio Gonzalez-Gonzalez[3,6], Devin Leake[7], Christopher H Contag[3] and Roger L Kaspar[1]

Despite the development of potent siRNAs that effectively target genes responsible for skin disorders, translation to the clinic has been hampered by inefficient delivery through the stratum corneum barrier and into the live cells of the epidermis. Although hypodermic needles can be used to transport siRNA through the stratum corneum, this approach is limited by pain caused by the injection and the small volume of tissue that can be accessed by each injection. The use of microneedle arrays is a less painful method for siRNA delivery, but restricted payload capacity limits this approach to highly potent molecules. To address these challenges, a commercially available motorized microneedle array skin delivery device was evaluated. This device combines the positive elements of both hypodermic needles and microneedle array technologies with little or no pain to the patient. Application of fluorescently tagged self-delivery (sd)-siRNA to both human and murine skin resulted in distribution throughout the treated skin. In addition, efficient silencing (78% average reduction) of reporter gene expression was achieved in a transgenic fluorescent reporter mouse skin model. These results indicate that this device effectively delivers functional sd-siRNA with an efficiency that predicts successful clinical translation.

Molecular Therapy—Nucleic Acids (2013) **2**, e129; doi:10.1038/mtna.2013.56; published online 22 October 2013
Subject Category: siRNAs, shRNAs, and miRNAs; therapeutic proof-of-concept

Introduction

Of the 7,000 known monogenic disorders, approximately 20% affect the skin.[1,2] While most of these diseases are individually rare, together they represent a significant healthcare burden and afflict up to 1% of the human population. For the vast majority of these disorders, there are no effective treatments that target the genetic basis of the disease. Nucleic acid-based therapies, including siRNAs, are being actively pursued as a means of selectively modifying the expression of disease-causing genes.[3] While traditional "small molecule" approaches to drug development have been a successful model for large pharmaceutical companies, the high cost of development (on the order of $1 billion) and the long development time (10–12 years) preclude practical application of this conventional strategy to rare disorders that affect small number of patients.[4] Identification and use of potent and selective siRNAs[5,6] with limited off-target and immunostimulatory activities is now routine in many laboratories and may offer a more efficient route to drug development for rare disorders.

The primary challenge to translating siRNA-based skin therapeutics to the clinic is the development of effective delivery systems. Substantial effort has been invested in a variety of skin delivery technologies with limited success.[7] In a clinical study in which skin was treated with siRNA, the exquisite pain associated with the hypodermic needle injection precluded enrollment of additional patients in the trial,[8] highlighting the need for improved, more "patient-friendly" (*i.e.*, little or no pain) delivery approaches.

Microneedles represent an efficient way to deliver large charged cargos including siRNAs across the primary barrier, the stratum corneum, and are generally regarded as less painful than conventional hypodermic needles.[9–11] Motorized "stamp type" microneedle devices, including the motorized microneedle array (MMNA) device used in this study, have been shown to be safe in hairless mice studies[11] and cause little or no pain as evidenced by (i) widespread use in the cosmetic industry and (ii) limited testing in which nearly all volunteers found use of the device to be much less painful than a flushot (TransDerm, data on file), suggesting siRNA delivery using this device will result in much less pain than was experienced in the previous clinical trial using hypodermic needle injections.[8]

In this work, we evaluated the ability of the MMNA device to deliver functional siRNA to transgenic reporter mouse skin. Reporter gene expression in these mice is limited to the epidermis,[12] mimicking monogenic epidermal disorders such as pachyonychia congenita and epidermolysis bullosa simplex. This device utilizes an array of fine steel needles, which oscillate in a piston-like fashion, to deliver materials into the tissue. The piston motion is adjustable, with regard to speed and depth, for the purpose of optimizing delivery of the drug through the stratum corneum to the targeted cells. In the cases where deposition of drug is targeted to the epidermis, delivery occurs with little or no pain as the needles to not penetrate sufficiently deep to trigger pain nerve bundles. We reasoned that

[1]TransDerm, Santa Cruz, California, USA; [2]Current address: University of Dundee, Dundee, UK; [3]Department of Pediatrics, Radiology, and Microbiology & Immunology, Stanford University School of Medicine, Stanford, California, USA; [4]Current address: Weill Cornell Medical College, New York, New York; [5]Department of Pathology, Yale University School of Medicine, New Haven, Connecticut, USA; [6]Current address: The Andalusian Centre for Nanomedicine and Biotechnology, BIONAND, Malaga, Spain; [7]Thermo Fisher Scientific, Dharmacon Products, Lafayette, Colorado, USA Correspondence: Roger L Kaspar, TransDerm, 2161 Delaware Ave, Suite D, Santa Cruz, California 95060, USA. E-mail: Roger.Kaspar@TransDermInc.com
Keywords: gene inhibition; nucleic acid therapeutics; reporter genes; siRNA delivery
Received 16 April 2013; accepted 8 August 2013; advance online publication 22 October 2013. doi:10.1038/mtna.2013.56

this tool could effectively be used to transit the stratum corneum and deposit self-delivery (sd)-siRNA into the epidermis, wherein the sd-siRNA would be taken up by resident cells. We have used fluorescently tagged sd-siRNA to monitor delivery to both mouse and human skin and have evaluated the ability of sd-siRNA to specifically inhibit reporter gene expression in the skin of a transgenic reporter mouse model.

Results

Despite the promise of siRNAs as therapeutics for skin disorders, a major obstacle has been delivery of these molecules through the stratum corneum barrier due to their size (~13,000 MW) and polyanionic nature. The MMNA device used in this study is available commercially (see Materials and Methods) and has the potential to deliver a variety of molecules across the stratum corneum through direct penetration using oscillating needles that are provided as a single use, sterile disposable cartridge (**Figure 1**).[9,10]

Delivery of sd-siRNA cargo into the epidermis using the MMNA device

As the device operates, liquid from the reservoir (**Figure 1**) is carried by the moving needles into the skin to preset depths. The oscillation of needles (up to 100 times per second) is used to penetrate the stratum corneum and deliver the therapeutic to the target sites by either deposition of the material that is coated on the needles or by the formation of channels through which liquid can penetrate. To determine the volume of solution that potentially can be delivered to skin, the MMNA cartridge was loaded with 50, 100, 200, or 300 µl of phosphate-buffered saline (PBS). After application to murine flank skin, the solution remaining in the cartridge and on the surface of the skin was collected and measured to calculate the total volume delivered to the tissue. Loading of 50 µl of solution into the device resulted in an average of 16 µl being delivered to the skin. A maximum deliverable volume of 40 µl was reached when a volume of 100 µl or greater was loaded (**Supplementary Figure S1a**). As the depth of needle penetration can be adjusted, this device has the potential to deliver cargo to skin with thicknesses ranging from mouse flank skin (<50 µm) to much thicker human plantar skin (>1 mm). Furthermore, the ability to adjust penetration depth allows for selective deposition of the therapeutic in the epidermis, avoiding the pain nerve fibers that are prevalent in the dermis.[9,10] At the "0.1" setting (100 micron nominal) used in this study, no obvious signs of pain were observed during or following treatment of mice (*e.g.*, no noticeable increased licking or twitching of the treated area).[13,14]

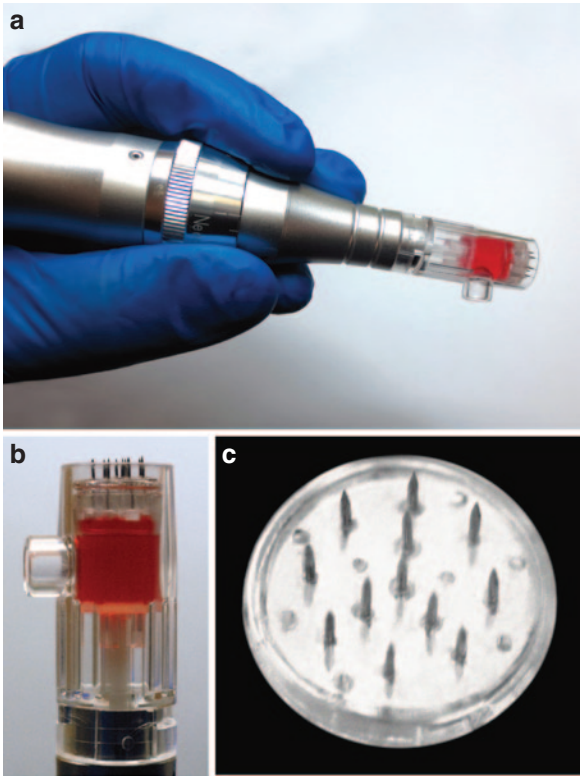

Figure 1 Handheld motorized microneedle array device. (**a**) The inner reservoir of the motorized microneedle array cartridge contains 300 µl of a red dye solution for visualization. (**b**) The needles can be adjusted for penetration depth and are set here at 0.1 mm to protrude slightly beyond the edge of the chamber. (**c**) Channels located between the needles allow flow of solution onto the surface of the skin during treatment.

To evaluate nucleic acid delivery by intravital imaging, 50 µl of 0.1 mg/ml fluorescently tagged sd-siRNA (Cy3-Accell siRNA, see Materials and Methods) were administered to murine flank skin with the MMNA device. As a control, 16 µl of the same solution was injected intradermally using a hypodermic needle adjacent to the treated site. *In vivo* imaging revealed similar fluorescence intensities at both sites, suggesting that equal amounts of sd-siRNA were delivered under these conditions by both methods (**Supplementary Figure S1b)**. The punctate distribution pattern observed upon MMNA treatment of mouse flank skin (**Supplementary Figure S1b**) is probably due to the siRNA initially delivered where the microneedles penetrate the skin.

To visualize sd-siRNA distribution after delivery through the stratum corneum barrier, mouse skin which had been treated with fluorescently tagged sd-siRNA was analyzed by fluorescence microscopy. Delivery with the MMNA device resulted in a gradient of fluorescently tagged sd-siRNA distribution throughout the treated area of the skin with peak intensities observed at the sites of needle penetration (**Figure 2a**). Of note, significant fluorescent signal was observed at sites lateral to the needle tract and within the epidermis. The morphology, number, and size of cells suggest that the labeled siRNA is associating with keratinocytes (**Figure 2b**,**c**). Intradermal injection of the fluorescently tagged sd-siRNA resulted in comparable distribution of signal throughout the dermis and epidermis.

The distribution of labeled sd-siRNA in human skin was similarly analyzed (**Figure 2d**). As in mouse skin, the fluorescent signal was observed in a gradient pattern from the site of needle penetration including lateral distribution through the epidermis (**Figure 2e**,**f**). In contrast to the distribution

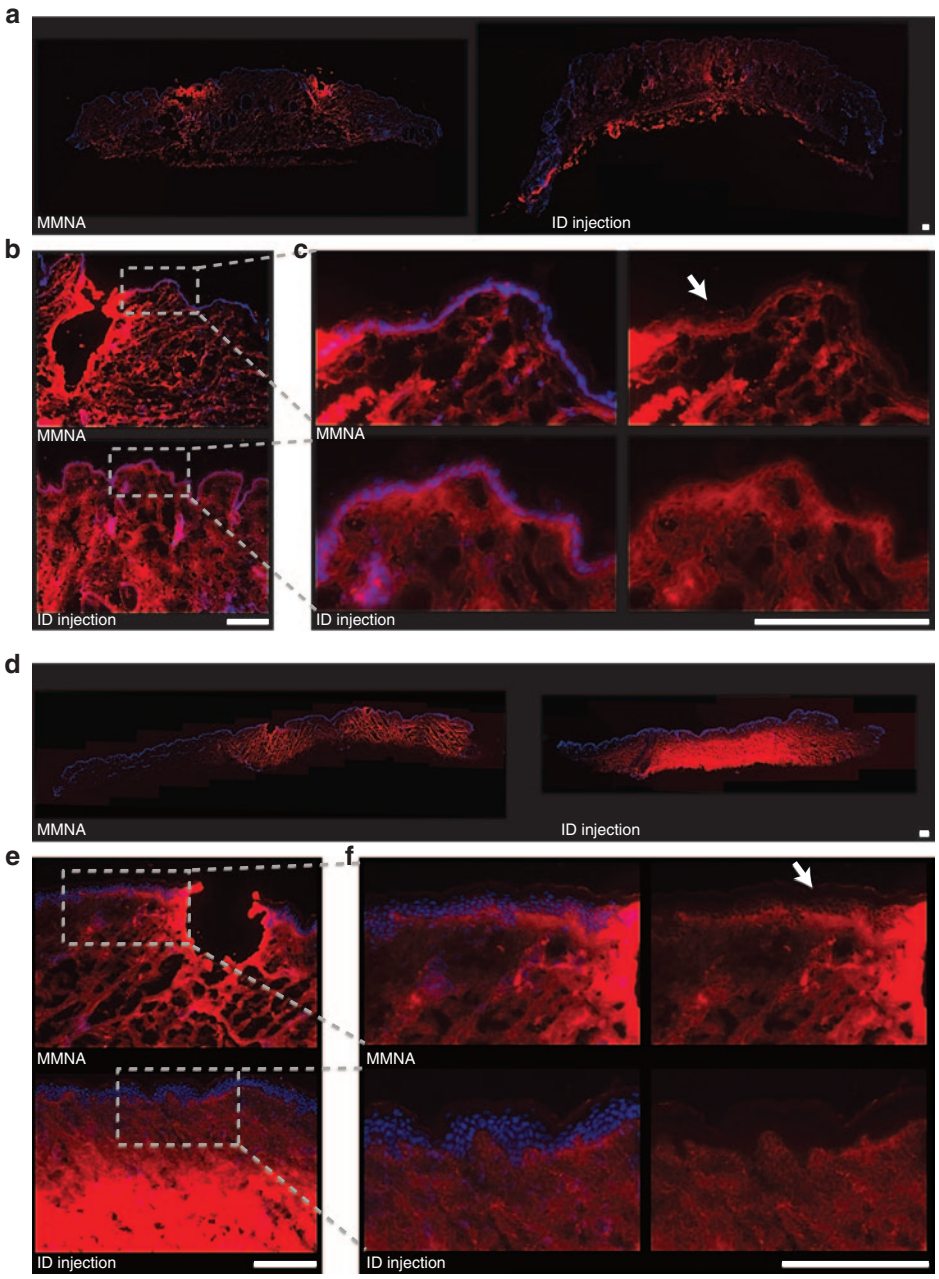

Figure 2 Cy3-labeled sd-siRNA distribution in mouse and human skin. Mouse or human skin was treated with the motorized microneedle array device loaded with 50 µl of 0.1 mg/ml Cy3-labeled sd-siRNA and intradermally injected as described below. After a 1-hour incubation, skin was collected, frozen in optimum cutting temperature (OCT) compound, and sectioned (10 µm). (**a**) Sections of hairless mouse flank skin in which breaches in the epidermis are shown in their entirety using a ×5 objective. Intradermally injected skin (16 µl of 0.1 mg/ml Cy3-labeled sd-siRNA) was sectioned to the center of the injection site and similarly displayed. The individual images were stitched together using ICE software. (**b**) Magnification (×10) of treated skin. (**c**) Further magnification of images from (**b**) shows diffusion of the Cy3-labeled sd-siRNA in the epidermis originating from the needle penetration site (arrow). Left panels: 4′,6-diamidino-2-phenylindole and Cy3 overlay; right panels: Cy3 alone. (**d**) Distribution of fluorescently labeled sd-siRNA in human abdominoplasty skin. Skin breaches due to penetration of the motorized microneedles are seen in their entirety using a ×5 objective. Intradermally injected skin (50 µl of 0.1 mg/ml Cy3-labeled sd-siRNA) was similarly sectioned and imaged. (**e**) Magnification of treated skin. (**f**) Further magnification of the images from (**e**) shows diffusion of the Cy3-labeled sd-siRNA in the epidermis originating from the needle penetration site (arrow), whereas low levels of fluorescence are observed in the epidermis following intradermal injection. Left panels: 4′,6-diamidino-2-phenylindole, and Cy3 overlay; right panels: Cy3 alone. Nuclei are visualized by DAPI (blue). Scale bar = 200 µm.

pattern observed upon intradermal injection in mouse flank (**Figure 2c**), less labeled siRNA was detected in the epidermis of human skin following intradermal injection with a hypodermic needle (**Figure 2e,f**), consistent with previous experiments in both human abdominal explant skin and mouse footpad skin (unpublished data).

Distribution of fluorescently tagged sd-siRNA following MMNA-assisted delivery in human skin by intravital confocal microscopy

The distribution of labeled sd-siRNA was further investigated in human skin using confocal fluorescence microscopy. Cy3-labeled sd-siRNA was administered to a fresh human skin sample and imaged by intravital confocal imaging (**Figure 3**). The reflectance images show the penetration site of a single needle from the array (**Figure 3a**). Fluorescence imaging shows radial distribution of signal from the needle penetration site (**Figure 3b**) and interaction with individual cells (**Figure 3c**). The full data set from the skin surface to a depth of 100 µm (imaged at 1 µm steps) is included as **Supplementary Video S1**.

Silencing of reporter gene expression in transgenic mouse epidermis

We have previously reported silencing of a fluorescent reporter gene in a transgenic (tg) mouse skin model (tg-CBL/ humanized monster green fluorescent protein (hMGFP)) after administration of unmodified and sd-CBL3 siRNA by intradermal injection[12] and microneedle application,[15] respectively. To evaluate the ability of the MMNA device to deliver functional CBL3 sd-siRNA in this model, hairless tg-CBL/hMGFP mouse flank skin was treated (n = 3) and reporter gene expression was analyzed. CBL3 sd-siRNA was administered to flank skin six times over a period of 11 days with the device. Mice were imaged with intravital imaging tools during the treatment regiment;

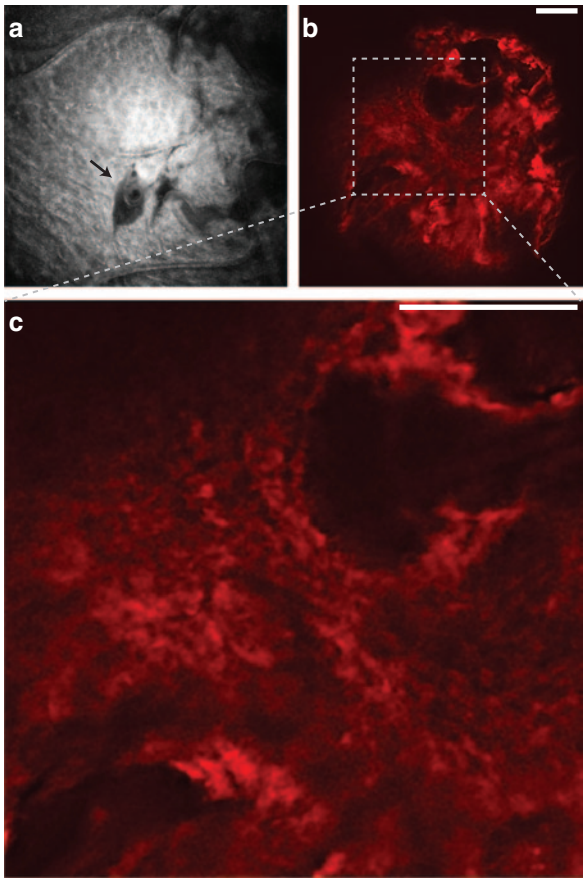

Figure 3 Confocal fluorescence imaging of Cy3-labeled sd-siRNA in human skin. Following motorized microneedle array delivery (30–60 minutes) of 100 µl of 0.5 mg/ml Cy3-labeled sd-siRNA (in phosphate-buffered saline) to excised human facial skin, siRNA distribution was imaged (reflectance and red fluorescence) with a modified Lucid VivaScope (see Materials and Methods). (**a**) Reflectance imaging at 29-µm depth shows the primary penetration site for this individual needle (note arrow). (**b**) Fluorescence imaging at 59-µm depth shows the diffusion of labeled sd-siRNA through the epidermis. (**c**) Magnification of the boxed region in (**b**) shows the interaction of the labeled sd-siRNA with individual cells. Scale bar = 100 µm.

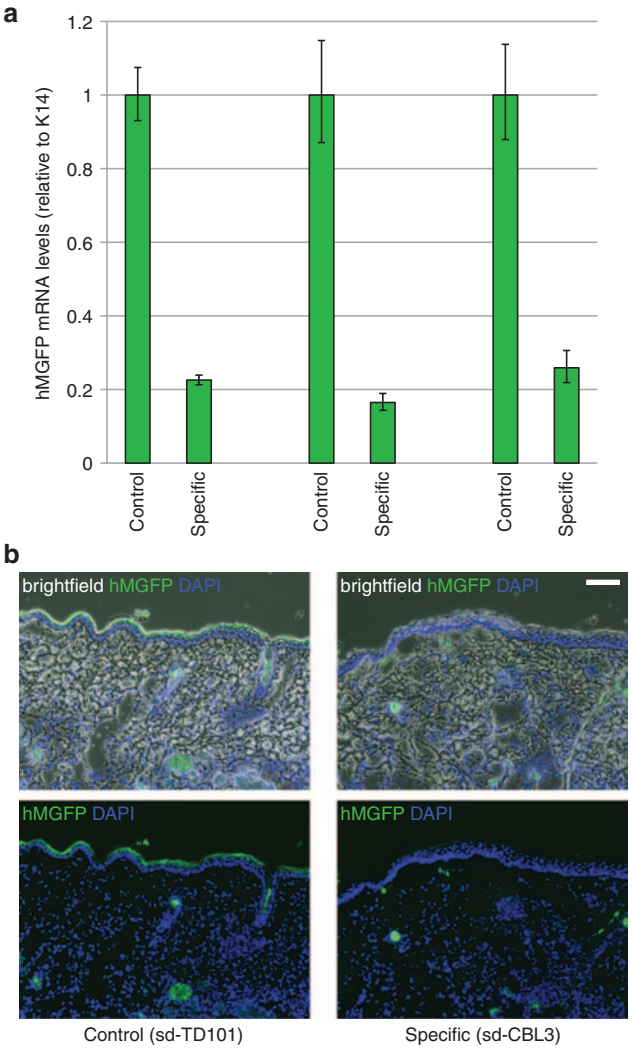

Figure 4 Delivery of sd-siRNA strongly inhibits targeted reporter gene expression. Hairless tg-CBL/hMGFP mouse flank skin (n = 3) was treated on days 0, 2, 4, 6, 8, and 10 with the MMNA device loaded with 100 µl of 5 mg/ml CBL3 sd-siRNA or nonspecific control sd-siRNA (sd-TD101). The mouse skin was marked to allow the same area of the flank to be treated for each administration. On day 11, the mice were killed and the treated skin was excised for RTqPCR analysis and fluorescence imaging. (**a**) Total RNA was isolated from the epidermis of the excised skin, reverse transcribed, and reporter (CBL/hMGFP) mRNA levels (relative to K14) were quantified in triplicate by qPCR. Bars indicate standard error. (**b**) Representative fluorescence images (bottom) with bright field overlay (top) of frozen skin sections (10 µm) prepared from treated mice show inhibition of hMGFP fluorescence signal in the skin treated with specific sd-siRNA over control sd-siRNA. Nuclei are visualized by DAPI (blue). Scale bar is 100 µm.

however, the hMGFP signal was not sufficiently strong to reproducibly visualize and quantify differences between sites treated with specific siRNA and nonspecific control siRNA. Mice were killed the day after the last treatment, and flank skin was excised for RNA isolation and histology. Reporter mRNA (CBL/hMGFP) levels in the epidermis were measured by RT-qPCR (**Figure 4a**). A significant reduction (78±5%) of reporter expression was detected in the epidermis of skin treated with the specific CBL3 sd-siRNA compared with the contralateral flank skin treated with nonspecific control (TD101 sd-siRNA). This experiment was repeated comparing CBL3 sd-siRNA with an additional nonspecific sd-siRNA control (targets human, but not mouse, CD44), and similar results were observed (data not shown). The decreased hMGFP levels were corroborated by fluorescence microscopy of CBL3 sd-siRNA-treated skin compared with control sd-siRNA treatment (**Figure 4b**). Fluorescence images of hMGFP were overlaid with 4′,6-diamidino-2-phenylindole (DAPI) and bright field images to locate the basal layer and stratum corneum, respectively.

Histological analysis of treated skin

To assess potential tissue damage due to penetration of the array microneedles alone versus inflammation caused by deposition of sd-siRNA, PBS, or sd-siRNA (in PBS) was administered to hairless tg-CBL/hMGFP mice with the MMNA device. The skin was harvested 24 hours after treatment and immediately fixed in formalin and embedded in paraffin. Histology of the treated skin revealed areas consistent with needle penetration and associated skin damage (**Supplementary Figure S2** shows a representative image of mouse skin treated with CBL3 sd-siRNA). Acute inflammation was observed with a prominent polymorphonuclear infiltrate in the papillary dermis extending down into, but not through, the reticular dermal layer, primarily at the site of needle penetration through the epidermis but also throughout the dermis. Scattered macrophages and chronic inflammatory cells were also present, consistent with classic wound healing, as would be expected from a standard hypodermic needle injection. Inflammation was generally localized around wounded regions. There were no visual differences in wound response in skin treated with vehicle alone as compared with skin treated with TD101 or CBL3 sd-siRNA (data not shown), suggesting that the observed acute inflammation is not due to the presence of sd-siRNA.

Discussion

Due to its accessibility, skin is an attractive target for siRNA therapeutics, and direct injection of "naked" nucleic acids has been suggested as a simple, safe, and efficient delivery method.[16] However, direct injections are limited to a highly localized region of the epidermis coincident with the injection site, and large number of injections may be needed to achieve the uniform delivery required for a favorable therapeutic outcome.[8,12,17] Indeed, although efficacy was observed in the first clinical trial using intradermally injected siRNA (TD101 targets a single nucleotide keratin 6a mutation responsible for pachyonychia congenita),[8] the observed improvement was limited to the area immediately surrounding the plantar injection site. The positive outcome yielded a significant proof-of-principle result, but due to the limited size of the treatment area, did not appreciably reduce the patient pain levels for the entire foot. Furthermore, the intradermal injections of either siRNA or vehicle alone were accompanied by severe pain,[8] necessitating nerve blocks as well as oral pain medication before treatment. This pain was probably due, at least in part, to the large volume (up to 2 ml) of drug injected into the lesion. After the trial, we reported that part of the mechanism for efficient delivery of the unmodified siRNA was likely due to the high pressure resulting from the injection,[18] similar to what occurs in hydrodynamic delivery to other organs including liver by tail vein injections.[19] The high pressure required for siRNA delivery was likely at least partially responsible for the intense pain experienced with these injections, which has led us to refocus on developing alternative "patient-friendly" (*i.e.*, little or no pain) delivery technologies.

For functional delivery, siRNA must not only transit the stratum corneum barrier, but also be internalized into cells in a manner that allows for incorporation into the RNA-induced silencing complex (RISC).[20] In addition to direct injection with a hypodermic needle, multiple physical approaches have been evaluated that reportedly facilitate delivery of nucleic acids across the stratum corneum barrier including ultrasound,[21] erbium:YAG laser,[22] gene gun,[23] iontophoresis,[24] electroporation,[25–27] microneedles,[15,28–30] and now motorized microneedles. As mentioned above, however, unmodified nucleic acids are not normally taken up by keratinocytes in the absence of transfection agents unless the administration is accompanied with pressure ("pressure-fection").[18] Covalent "sd" siRNA modifications (including Dharmacon's Accell modifications) facilitate cellular uptake *in vitro* and *in vivo* without the need for transfection reagents.[15,20,30] We previously reported that administration of sd-siRNA by dissolvable microneedle arrays could reduce target gene expression up to 50% in both mouse[15] and human[30] skin models. The nearly 80% average reduction in target gene expression reported herein delivering sd-siRNAs with the MMNA device exceeds the threshold of 50% target gene inhibition, which we hypothesize is the minimum expected to achieve a clinical effect,[8,31,32] and warrant additional study for translation to the clinic.

The results presented here indicate that the MMNA device effectively delivers siRNA to relevant regions of the skin with an efficiency (up to 80% inhibition) that, if translatable to human subjects, may offer relief to patients suffering from debilitating monogenic skin disorders. In a separate study using this same transgenic skin reporter mouse model,[12] direct injection of unmodified siRNA with a hypodermic needle resulted in 33% decrease in reporter gene expression. No head-to-head direct studies to compare sd-siRNA delivery by intradermal injection and MMNA-mediated delivery have been performed as our goal is to develop a viable clinical option, and the pain associated with intradermal injection, at least in pachyonychia congenita patients, precludes this method of administration. Although comparison of the pain associated with treatment with the MMNA device with intradermal injection was not a part of this study, others have reported significantly decreased pain associated with microneedles as compared with intradermal injections in human studies.[9,10] Furthermore, the observation that the MMNA device is used in the cosmetic industry suggests it may have a sufficient safety profile,[11] and may provide a

strong alternative to traditional microneedles and hypodermic needle injections.

Materials and methods

Animals. SIM: (HRS) hr/hr hairless mice (6–8 weeks old) were purchased from Simonsen Laboratories (Gilroy, CA). Hairless (SKH1) tg-CBL/hMGFP mice were generated by breeding tg-CBL/hMGFP mice[12] on a hairless background (SKH1; Charles River Laboratories, Wilmington, MA)[28] and maintained at Stanford University. Animals were treated under isofluorane anesthesia according to the guidelines of the National Institutes of Health, TransDerm and Stanford University.

siRNA. "Self-delivery"-specific (CBL3)[15] and -nonspecific (TD101,[20] CD44,[30] and nontargeting Cy3-labeled) siRNAs containing Dharmacon-proprietary modifications (Accell, Wilmington, MA) were synthesized by Thermo Fisher Scientific, Dharmacon Products (Lafayette, CO); Accell siRNAs are available commercially from this source.

Delivery of sd-siRNA by the Tri-M MMNA device. The MMNA device (marketed as Triple-M or Tri-M by Bomtech Electronic Co, Seoul, South Korea) was adapted for delivery of siRNA to mouse and human skin. sd-siRNA solution (up to 300 µl) was introduced into the chamber of the disposable Tri-M needle cartridge (Bomtech), which was set to a depth of 0.1 mm. For treating mice, a fold of skin was laid flat on a rigid support positioned directly under the cartridge. Once oriented vertically and perpendicular to the fold of skin, the device was powered on to the highest speed and held in place for 10 seconds. For treating human skin, deidentified skin (obtained immediately following surgical procedures) was manually stretched and pinned to a cork platform before treatment as described above. All intradermal injections[18] were performed using an insulin syringe with a 28-gauge 0.5-inch needle.

Histological analysis of fluorescently labeled sd-siRNA distribution in murine and human skin. Cy3-labeled nontargeting sd-siRNA was loaded into the chamber of the MMNA device. Mouse flank skin or deidentified human abdominal skin was treated as described above and imaged with an IVIS Lumina II imaging system (Xenogen product from Perkin Elmer, Alameda, CA) using the 535-nm excitation and DsRed emissions settings. The data were quantified using Living Image software (Perkin Elmer) and presented as an overlay with the bright field data. Fluorescent background from an untreated area of the same animal or tissue sample was subtracted and values were reported as radiant efficiency. Skin was then embedded in OCT, sectioned (10 µm), and mounted with Hydromount (National Diagnostics, Atlanta, GA) containing 1 µg/ml DAPI for analysis by fluorescence microscopy using a Zeiss Axio Observer inverted fluorescence microscope equipped with Cy3 and DAPI filter sets (Carl Zeiss Microscopy, Thornwood, NY). Images were "stitched" together using Microsoft Image Composite Editor (ICE).

Confocal microscopy of fluorescently labeled sd-siRNA distribution in human skin. Cy3-labeled nontargeting sd-siRNA was administered to deidentified human skin from a rhytidectomy procedure. The skin was treated as described above and imaged using a modified (for fluorescence) Lucid VivaScope 2500 System (Lucid, Rochester, NY),[29] which was further enhanced by the manufacturer to achieve dual fluorescence capabilities by the addition of a MiniGreen 532-nm laser (Snake Creek Lasers, Hallstead, PA). Briefly, image z-stacks were generated by image acquisition at successive 1 µm z-depths using native VivaScan software (v. VS008.01.09) and postprocessed using public domain Fiji Java-based image processing software.[33] Images were acquired in reflectance mode using the 658-nm laser source with an "open" emission window. Duplicate fluorescent images were acquired using the 532-nm excitation laser and the 607/70-nm emission filter.

To increase the effective resolution of the VivaScope images, 10 images were taken at each z-step, and these 10 image sets were averaged to produce z-step-averaged images, resulting in the final image stack. Because *in vivo* imaging is influenced by respiration and other minor subject motion, successive frames were coregistered using an affine transform[34] (distributed with Fiji software as the StackReg plug-in) before any frame averaging. Fluorescence images were false colored according to the channel used for acquisition.

Delivery of functional sd-siRNA and analysis of gene silencing. Anesthetized hairless tg-CBL/hMGFP mice were treated with sd-siRNA as described above. The day following the last treatment, mice were euthanized and the treated area was excised for analysis by both fluorescence microscopy and RTqPCR as described in [12] with the following modifications. For RTqPCR, the epidermis was separated from the dermis by incubation in dispase II (0.2 µm filtered 10 mg/ml in PBS, Roche, Indianapolis, IN) for 2–4 hours at 21 °C before RNA isolation from the epidermis only.

Histology. Hairless tg-CBL/hMGFP mice were treated with the MMNA device containing either PBS vehicle or CBL3 or TD101 sd-siRNA (in PBS) as described above. The skin was harvested 24 hours after treatment and immediately fixed in 10% neutral buffered formalin (Thermo Scientific, Kalamazoo, MI). Paraffin-embedded tissues were sectioned (5 µm) and stained with hematoxylin and eosin using conventional methods and imaged by standard microscopy.

Supplementary material

Figure S1. Motorized microneedle array delivery efficiency.
Figure S2. Histological analysis of skin following administration of sd-siRNA with the MMNA device.

Acknowledgments. We thank Leonard Milstone (Yale University) for stimulating discussions and providing feedback on the manuscript. We acknowledge Conor Cox for technical assistance and Andrea Burgon for assistance with figures. This study was funded in part by grants from the National Institutes of Health from NIAMS (RC2AR058955 [RLK and CHC]) and by unrestricted gifts from the Chambers Family Foundation (CHC). We are grateful for Javier Serrato (Medicol USA) for the suggestion to evaluate the Tri-M device.

1. <www.ncbi.nlm.nih.gov/entrez/query.fcgi?db=OMIM>.
2. <http://rarediseases.info.nih.gov/Resources/Rare_Diseases_Information.aspx>.
3. Burnett, JC and Rossi, JJ (2012). RNA-based therapeutics: current progress and future prospects. *Chem Biol* **19**: 60–71.
4. Kaspar, RL (2005). Challenges in developing therapies for rare diseases including pachyonychia congenita. *J Investig Dermatol Symp Proc* **10**: 62–66.
5. McLean, WH and Moore, CB (2011). Keratin disorders: from gene to therapy. *Hum Mol Genet* **20**(R2): R189–R197.
6. Rodriguez-Lebron, E and Paulson, HL (2006). Allele-specific RNA interference for neurological disease. *Gene Ther* **13**: 576–581.
7. Kaspar, RL, McLean, WH and Schwartz, ME (2009). Achieving successful delivery of nucleic acids to skin: 6th Annual Meeting of the International Pachyonychia Congenita Consortium. *J Invest Dermatol* **129**: 2085–2087.
8. Leachman, SA, Hickerson, RP, Schwartz, ME, Bullough, EE, Hutcherson, SL, Boucher, KM *et al.* (2010). First-in-human mutation-targeted siRNA phase Ib trial of an inherited skin disorder. *Mol Ther* **18**: 442–446.
9. Gill, HS, Denson, DD, Burris, BA and Prausnitz, MR (2008). Effect of microneedle design on pain in human volunteers. *Clin J Pain* **24**: 585–594.
10. Haq, MI, Smith, E, John, DN, Kalavala, M, Edwards, C, Anstey, A *et al.* (2009). Clinical administration of microneedles: skin puncture, pain and sensation. *Biomed Microdevices* **11**: 35–47.
11. Park, KY, Jang, WS, Lim, YY, Ahn, JH, Lee, SJ, Kim, CW *et al.* (2013). Safety evaluation of stamp type digital microneedle devices in hairless mice. *Ann Dermatol* **25**: 46–53.
12. Gonzalez-Gonzalez, E, Ra, H, Hickerson, RP, Wang, Q, Piyawattanametha, W, Mandella, MJ *et al.* (2009). siRNA silencing of keratinocyte-specific GFP expression in a transgenic mouse skin model. *Gene Ther* **16**: 963–972.
13. Dubuisson, D and Dennis, SG (1977). The formalin test: a quantitative study of the analgesic effects of morphine, meperidine, and brain stem stimulation in rats and cats. *Pain* **4**: 161–174.
14. Jourdan, D, Ardid, D, Bardin, L, Bardin, M, Neuzeret, D, Lanphouthacoul, L *et al.* (1997). A new automated method of pain scoring in the formalin test in rats. *Pain* **71**: 265–270.
15. Gonzalez-Gonzalez, E, Speaker, TJ, Hickerson, RP, Spitler, R, Flores, MA, Leake, D *et al.* (2010). Silencing of reporter gene expression in skin using siRNAs and expression of plasmid DNA delivered by a soluble protrusion array device (PAD). *Mol Ther* **18**: 1667–1674.
16. Hengge, UR, Walker, PS and Vogel, JC (1996). Expression of naked DNA in human, pig, and mouse skin. *J Clin Invest* **97**: 2911–2916.
17. Leachman, SA, Hickerson, RP, Hull, PR, Smith, FJ, Milstone, LM, Lane, EB *et al.* (2008). Therapeutic siRNAs for dominant genetic skin disorders including pachyonychia congenita. *J Dermatol Sci* **51**: 151–157.
18. González-González, E, Ra, H, Spitler, R, Hickerson, RP, Contag, CH and Kaspar, RL (2010). Increased interstitial pressure improves nucleic acid delivery to skin enabling a comparative analysis of constitutive promoters. *Gene Ther* **17**: 1270–1278.
19. Liu, F, Song, Y and Liu, D (1999). Hydrodynamics-based transfection in animals by systemic administration of plasmid DNA. *Gene Ther* **6**: 1258–1266.
20. Hickerson, RP, Flores, MA, Leake, D, Lara, MF, Contag, CH, Leachman, SA *et al.* (2011). Use of self-delivery siRNAs to inhibit gene expression in an organotypic pachyonychia congenita model. *J Invest Dermatol* **131**: 1037–1044.
21. Tran, MA, Gowda, R, Sharma, A, Park, EJ, Adair, J, Kester, M *et al.* (2008). Targeting V600EB-Raf and Akt3 using nanoliposomal-small interfering RNA inhibits cutaneous melanocytic lesion development. *Cancer Res* **68**: 7638–7649.
22. Lee, WR, Shen, SC, Zhuo, RZ, Wang, KC and Fang, JY (2009). Enhancement of topical small interfering RNA delivery and expression by low-fluence erbium:YAG laser pretreatment of skin. *Hum Gene Ther* **20**: 580–588.
23. Arora, A, Prausnitz, MR and Mitragotri, S (2008). Micro-scale devices for transdermal drug delivery. *Int J Pharm* **364**: 227–236.
24. Kigasawa, K, Kajimoto, K, Hama, S, Saito, A, Kanamura, K and Kogure, K (2010). Noninvasive delivery of siRNA into the epidermis by iontophoresis using an atopic dermatitis-like model rat. *Int J Pharm* **383**: 157–160.
25. Broderick, KE, Chan, A, Lin, F, Shen, X, Kichaev, G, Khan, AS *et al.* (2012). Optimized *in vivo* transfer of small interfering RNA targeting dermal tissue using *in vivo* surface electroporation. *Mol Ther Nucleic Acids* **1**: e11.
26. Nakai, N, Kishida, T, Shin-Ya, M, Imanishi, J, Ueda, Y, Kishimoto, S *et al.* (2007). Therapeutic RNA interference of malignant melanoma by electrotransfer of small interfering RNA targeting Mitf. *Gene Ther* **14**: 357–365.
27. Golzio, M, Mazzolini, L, Ledoux, A, Paganin, A, Izard, M, Hellaudais, L *et al.* (2007). *In vivo* gene silencing in solid tumors by targeted electrically mediated siRNA delivery. *Gene Ther* **14**: 752–759.
28. Chong, RH, Gonzalez-Gonzalez, E, Lara, MF, Speaker, TJ, Contag, CH, Kaspar, RL *et al.* (2013). Gene silencing following siRNA delivery to skin via coated steel microneedles: *In vitro* and *in vivo* proof-of-concept. *J Control Release* **166**: 211–219.
29. González-González, E, Kim, YC, Speaker, TJ, Hickerson, RP, Spitler, R, Birchall, JC *et al.* (2011). Visualization of plasmid delivery to keratinocytes in mouse and human epidermis. *Sci Rep* **1**: 158.
30. Lara, MF, González-González, E, Speaker, TJ, Hickerson, RP, Leake, D, Milstone, LM *et al.* (2012). Inhibition of CD44 gene expression in human skin models, using self-delivery short interfering RNA administered by dissolvable microneedle arrays. *Hum Gene Ther* **23**: 816–823.
31. Cao, T, Longley, MA, Wang, XJ and Roop, DR (2001). An inducible mouse model for epidermolysis bullosa simplex: implications for gene therapy. *J Cell Biol* **152**: 651–656.
32. Wong, P, Domergue, R and Coulombe, PA (2005). Overcoming functional redundancy to elicit pachyonychia congenita-like nail lesions in transgenic mice. *Mol Cell Biol* **25**: 197–205.
33. Schindelin, J, Arganda-Carreras, I, Frise, E, Kaynig, V, Longair, M, Pietzsch, T *et al.* (2012). Fiji: an open-source platform for biological-image analysis. *Nat Methods* **9**: 676–682.
34. Thévenaz, P, Ruttimann, UE and Unser, M (1998). A pyramid approach to subpixel registration based on intensity. *IEEE Trans Image Process* **7**: 27–41.

Supplementary Information accompanies this paper on the Molecular Therapy–Nucleic Acids website (http://www.nature.com/mtna)